1 Introduction

1.1 Introduction and Chapter Objectives

An adhesive is a material that can be used to join two or more other materials. Adhesive bonding is a method by which materials can be joined to generate assemblies. Adhesive bonding is an alternative to more traditional mechanical methods of joining materials, such as nails, rivets, screws, etc. Adhesive bonding is not a new joining method. Use of adhesives is described in ancient Egypt [1] and in the Bible [2]. Bommarito [3] describes recipes for adhesives that were formulated during the Middles Ages. One such recipe shows that people in the middle ages had an appreciation for the generation of composite materials as well as the use of "drying oils":

> *"Very Strong, Very Good Glue"*
>
> *"Take clay roof tiles and grind them to a fine powder using a flour grinder. Add a similar amount of iron rust, also ground to a fine powder. Add live lime in an amount equivalent to the clay and iron rust and incorporate the mixture with linseed oil. Use immediately to glue what you want as this glue is better when used fresh than otherwise".*

A "glue" is an adhesive that is formulated primarily from natural products. In common vernacular, the word "glue" is used interchangably with "adhesive". In addition, "glue" is also used as a verb. For example, one can "glue two or more things together" or "one can adhesively bond two or more things together". The former statement refers primarily to natural product adhesives while the latter refers to all adhesives. In this book, we use the terms adhesive and adhesive bonding and reserve the terms "glue" and "to glue" for natural product-based adhesives.

A major step in adhesive technology took place in the early 1900s with the advent of synthetically prepared adhesives. Thus, widespread use of adhesives as a joining medium is a relatively recent phenomenon.

All joining methods have their advantages and disadvantages and adhesive bonding is not an exception. This introductory chapter explores some of the positive and

negative features of adhesive bonding as a joining method. Exploring these features sets the stage for many of the chapters to follow. The objectives of this chapter are:

- to acquaint the reader with the basic definitions used in adhesion science
- to provide the reader with a basis for understanding the advantages and disadvantages of using adhesive bonding
- to discuss the place of adhesive technology in our economy and to provide examples of where adhesives are utilized
- to describe sources of information about adhesion and adhesives for those who are becoming practitioners of the art and science of adhesive bonding.

1.2 Basic Definitions

An assembly made by the use of an adhesive is called an *adhesive joint* or an *adhesive bond*. Solid materials in the adhesive joint other than the adhesive are known as the adherends. The phenomenon, which allows the adhesive to transfer a load from the adherend to the adhesive joint, is called *adhesion*. There is also the phenomenon of *abhesion*, which is the condition of having minimal adhesion. This property is important when an assembly is needed from which the adhesive can be removed on demand. Materials that exhibit abhesion are also known as *release materials* and they are used to make certain pressure-sensitive adhesive constructions. Pressure-sensitive adhesives are described in Chapter 10.

The actual strength of an adhesive joint is primarily determined by the mechanical properties of the adherends and the adhesive. The term we apply to the measured physical strength of an adhesive bond is *practical adhesion*. The primary purposes of this book are to describe the phenomenon of adhesion, to describe the chemistry and properties of adhesives and to discuss the current understanding of the relationship between practical adhesion, adhesion and the mechanisms of energy dissipation in the adhesive joint.

1.3 Advantages and Disadvantages of Adhesive Bonding

One major differentiation between an adhesive joint and a mechanically fastened joint is that in the second, a mechanical fastener must pierce the adherend in order to execute an assembly. When a mechanical fastener pierces an adherend, or if the adherend is pierced before the installation of a mechanical fastener, a hole is created in the adherend.

In Figure 1.1 we see two examples of an adherend. In Figure 1.1(a), the adherend is intact. If a load was applied to the adherend, the lines of force propagating through the adherend would be continuous. If instead, the adherend had a hole in it (such as depicted in Figure 1.1(b)), the lines of force could not be continuous through the adherend and would have to go around the hole. Thus, at the edges of the hole, the force experienced by the material is much larger than the force experienced by the material remote from the hole. The edges of the hole not only have to support the force that is applied to those edges, but also must support the force that should have been supported by the material that would have been in the hole. As we will find in Sections 2.4 and 3.5.1 on fracture mechanics, this situation is known as a *stress concentration*.

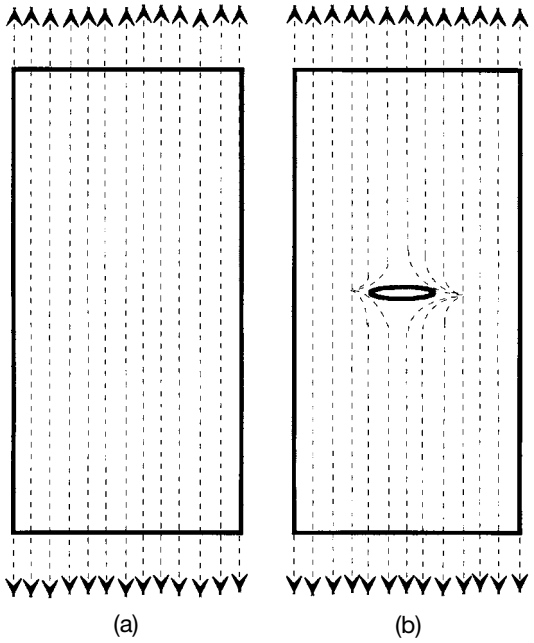

Figure 1.1 Diagram showing lines of force through a monolithic body (a) and a body containing an elliptical hole (b). The lines of force pass continuously through (a) but are unable to do so in (b). This results in a stress concentration at the edges of the elliptical hole

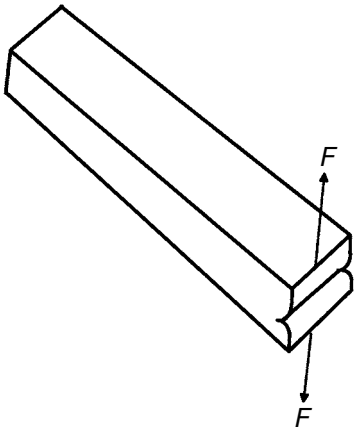

Figure 2.3
A material having a pre-existing crack along one of its edges is shown. A force is applied in a tensile fashion perpendicular to the crack. The material is said to be placed in "cleavage". Later in this book, we call this method of applying a load "Mode I Cleavage"

■ 2.3 Stress-Strain Plots and the Definition of Materials Property Parameters

2.3.1 Tensile Forces

In the tensile test described in the previous section, if the sample has a known cross sectional area, A, and F is the force applied by the tensile testing machine, then we define the *tensile stress*, σ, as

$$\sigma = \frac{F}{A} \tag{2.1}$$

The tensile stress is an important engineering concept in that the force F is applied across a specific cross sectional area of sample. Many different materials can have the same resistance to an applied force if the cross sectional area of the sample is the appropriate size. *Elongation* is the change in the length of the sample as the result of tensile forces. The elongation of the sample is defined in terms of the original dimensions of the specimen. Thus, if the original length of the sample is l_0 and the length (displacement) of the sample after a certain amount of tensile stress was applied is l, then we can define the term ε as follows:

$$\varepsilon = \left(l - l_0\right)/l_0 \tag{2.2}$$

where ε is known as the *engineering tensile strain*. It is important to note that the engineering tensile strain is a dimensionless number and is usually reported as a fraction or multiplied by 100 to obtain a percentage. This number is also sometimes reported as *elongation* in industry.

A *stress-strain plot* can be generated using a tensile testing machine. A specimen of known cross-sectional area is subjected to a tensile force and the elongation is measured, as shown in Figure 2.4. The tensile stress is plotted on the *y*-axis and the engineering tensile strain is plotted on the *x*-axis. At some temperature of test, many materials have stress-strain plots similar to that shown in Figure 2.4. Stress-strain plots for individual materials differ in the initial slope, in the position of the knee, in the length of the plateau portion of the curve, and in the *elongation at break* (also known as *strain at break*), which is indicated by the *X* in the plot. The slope of the initial part of the stress-strain plot is exceedingly important in both engineering and materials science. For most materials, the initial part of the stress-strain plot is linear, thus the relationship of stress and strain is as follows:

$$\sigma = E\,\varepsilon \tag{2.3}$$

where σ is the tensile stress, ε is the engineering tensile strain, and E is a constant.

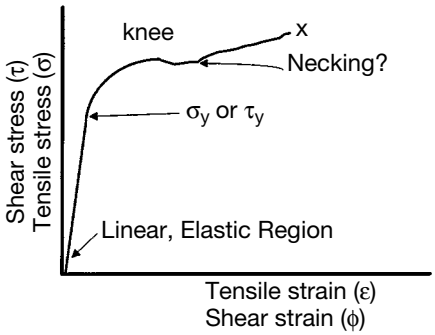

Figure 2.4 Schematic stress-strain curve. The engineering strain is plotted on the *x*-axis while the stress is plotted on the *y*-axis. The axes are labeled for either tensile or shear stress and strain. Similar curves, but with different actual values, will be measured under both types of application of force. The yield stress is shown as well as the failure at break (indicated by the "*X*")

This relationship should be familiar. It is simply a restatement of *Hooke's Law for Springs*, that the stress and the strain are proportional. The force applied to a spring and the resultant elongation are directly proportional. The proportionality constant is called the *spring constant*.

A spring is usually used as a model for materials that behave according to this equation. Materials that obey Hooke's law are known as *linear elastic* materials. The response is *linear* with increasing force. If the force is removed, the material returns *elastically* to its original state. Elasticity means that when load is removed from the material, it returns to its original shape and size without the loss of mechanical energy as heat. The factor E is known as the *tensile modulus* or *Young's*

modulus of the material in test. Since the engineering tensile strain is dimensionless, the Young's modulus has the units of stress, Pascal (Pa) in SI units and pounds per square inch (psi) in English units. Since the above equation, $\sigma = E\,\varepsilon$ expresses the relation between the stress and strain rather than force and displacement, Young's modulus is a materials parameter describing how a material reacts to a given tensile force. If the slope of the stress-strain plot is steep, then Young's modulus is high and a large tensile load must be applied to the sample to get a small elongation of the material. Materials that have a high Young's modulus are described as "stiff". Materials that have a low Young's modulus are described as "flexible". Table 2.1 provides a short list of well-known materials and a comparison of their Young's moduli.

Table 2.1 Young's Moduli and Poisson's Ratio of Some Well-Known Materials

Material	Young's modulus (Pascal = N/m^2)	Poisson's ratio
Aluminum	7×10^{10}	0.33
Mild steel	2.2×10^{11}	0.28
Silicon	6.9×10^{10}	
Glass	6×10^{10}	0.23
Poly(methyl methacrylate)	2.4×10^{9}	0.33
Polycarbonate	1.4×10^{9}	
Low density polyethylene	2.4×10^{8}	0.38
Natural rubber	2×10^{6}	0.49

As shown in Figure 2.4, for most materials there is a stress at which the stress-strain curve exhibits a "knee", known as the *yield stress* of the material. This parameter plays an important role in our understanding of resistance to crack propagation as well as one of the parameters necessary for the proper design of adhesive bonds. The tensile yield stress is given the symbol σ_y and it marks the stress or strain at which the material no longer follows Hooke's Law. After the yield stress is reached, the material is non-elastic and is said to have been *plastically deformed*. Plastic deformation is a sign that the material is absorbing energy. In some adhesive bond designs, the yield stress is used as the strength of the adhesive or the adherend. This criterion for bond design is often used since the designer wishes the adhesive bond to remain elastic under the design loads.

Not all materials display the plateau region shown in Figure 2.4. The plateau is seen in materials that "neck-in" or "draw down" as the sample elongates. Note that in the plateau region, the stress on the sample can actually decrease. Eventually, the material can no longer sustain the stress and it breaks. The stress at this point is known as the *stress at break* while the strain at this point is known as the *strain at break* or the *elongation at break* of the material. The *ultimate tensile strength* of

"flatwise" load on the core. When generating a honeycomb core containing adhesive bonds, the objective is to obtain good wetting of the core by the adhesive. This forces the failure to occur by ripping of the core rather than extraction of the core from the adhesive. In general, those adhesives with appropriate flow and the ability to climb the walls of the core provide flatwise tensile bonds which fail the core. This test is used in aerospace and allied industries.

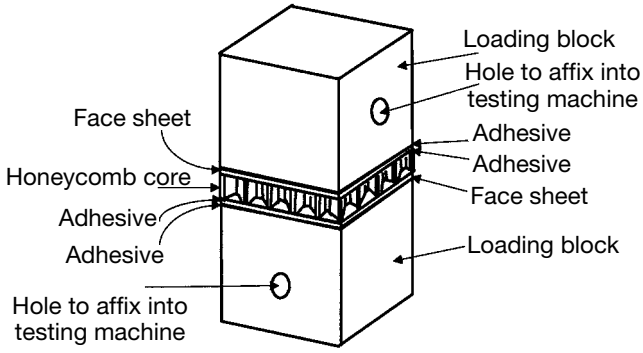

Figure 3.3 Diagram showing the construction of a flatwise tension specimen. The honeycomb core/face sheet sandwich is generated and then post-bonded to the tensile testing blocks. Pins to affix the specimen in the tensile testing machine are placed through the holes shown in the diagram. The specimen is tested to failure

■ 3.4 Shear Loading of Adhesive Bonds

In general, adhesives display their highest strength when loaded in shear. We have already described the loading conditions that place a material in shear in Chapter 2. If we look at Figure 2.2, we can imagine adherends attached to each of the faces of the block and we can imagine the block in Figure 2.2 to be the adhesive. There are many types of adhesive bond tests that place the adhesive in a state of shear such as those listed in Table 3.2. Indeed, most adhesive bonds used in actual structures are designed so that the adhesive is primarily in a state of shear. The reasons for this design choice become apparent as we begin to quote values of shear strength versus cleavage or peel strength for various adhesive types. Therefore, an understanding of shear loading is very important.

Table 3.2 ASTM Test Methods Pertaining to Determination of the Shear Properties of Adhesive Bonds

Test number	Title of test	Short description of test
D905	Test method for strength properties of adhesive bonds in shear by compression loading	2 × 4 in lumber is bonded and then tested by shearing the pieces in compression (the force is opposite to the sense shown in Figure 3.4)
D1002	Test method for strength properties of adhesives in shear by tension loading	Most used test method for evaluating adhesives, shown in Figure 3.4
D1780	Practice for conducting creep tests of metal-to-metal adhesives	D1002 shear specimens are subjected to a constant load and the movement of the adherends with respect to one another is determined
D2293	Test method for creep properties of adhesives in shear by compression loading (metal-to-metal)	A test similar to D1780 except that the constant load is in compression and is applied by a spring loaded device
D2294	Test method for creep properties of adhesives in shear by tension loading (metal-to-metal)	A test similar to D1780 except that the constant tensile load is applied by a spring-loaded device
D2295	Test method for strength of adhesives in shear by tension loading at elevated temperatures	A test similar to D1002 except that provisions are made for very high temperatures
D2339	Test method for strength properties of adhesives in two-ply wood construction in shear by tension loading	A no-filet test of plywood laminate shear strength. The plywood is made into a shear specimen by milling slots into the plywood
D2557	Test method for strength properties of adhesives in shear by tension loading in the temperature range of −267.8 to −55 °C	A test similar to D1002 except that provision is made for very low temperatures
D3163	Test method for determining the strength of adhesively bonded rigid plastic lap shear joints in shear by tension loading	A test similar to D1002 except that provisions are made for the adherends to be rigid plastics
D3164	Test method for determining the strength of adhesively bonded plastic lap-shear sandwich joints in shear by tension loading	A special test similar to D1002 except that a plastic is “sandwiched” between adhesive layers which are bonded to metal adherends. This test measures the adhesion of the adhesive to the plastic
D3528	Test method for strength properties of double lap shear adhesive joints by tension loading	A lap shear test which attempts to correct for the non-linearity of the loading path for D1002 specimens by having two adherends instead of one on one end of the bond

which we will discuss are only Mode I and the strain energy release rate is designated as $\mathcal{G}_{IC}$. When reading other literature on this topic, make note of the mode of fracture.

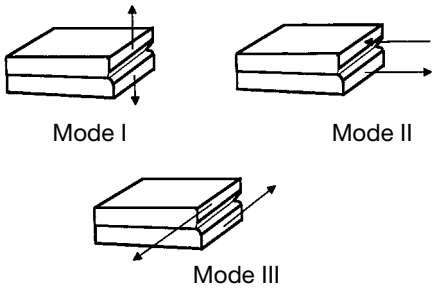

Figure 3.16 Schematic of the three modes of fracture. Mode I is known as cleavage. Mode II is known as shearing. Mode III is known as tearing. Note that Roman numerals are used to designate these modes

3.5.1.1 Double Cantilever Beam Specimens

The simplest fracture mechanics specimen to generate and analyze is the uniform, double cantilever beam specimen. This specimen is shown schematically in Figure 3.17 and described in ASTM D3433. In this specimen, the adherends are uniform in shape and profile. Their shape is usually square in cross section with dimensions of 1 × 1 in. Initially, a razor blade is driven into the end of the specimen to generate an end-crack. The blade is removed before testing. The load is applied at the end of the specimen in one of a number of ways. Most commonly, holes are drilled through the specimen as shown in Figure 3.17 and the specimen is fixed in a tensile testing machine by means of these holes. As the load is applied, the initial crack propagates. One parameter measured is the displacement of the specimen determined by the crosshead movement of the tensile testing machine. The second parameter measured is the crack length as a function of load. This measurement is substantially more difficult and is made by either fast photography or by affixing instruments to the adhesive bond. For example, one method is to paint the side of the bond with conductive paint at intervals and to measure the crack length by following the disruption of the conductive paths formed by the paint stripes.

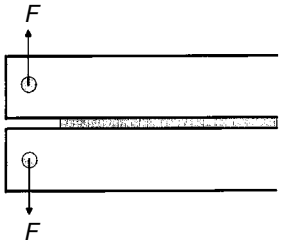

Figure 3.17
Double cantilever beam specimen

3.5.1.2 Linear Elastic Fracture Mechanics Applied to the Double Cantilever Beam Specimen

Rewriting Eq. (2.12) in terms of differential forces and displacement, we have

$$U_C = F\delta D + \frac{1}{2}\delta F\delta D - \frac{1}{2}\left(F\delta D + D\delta F + \delta F\delta D\right) \tag{3.31}$$

This equation can be simplified to be:

$$U_C = \frac{1}{2}\left(F\delta D - D\delta F\right) \tag{3.32}$$

Substituting Eq. (3.32) into Eq. (2.13) and Eq. (2.14), we have

$$\frac{1}{w}\frac{\delta}{\delta a}U_C = \frac{1}{2w}\left(F\frac{\delta D}{\delta a} - D\frac{\delta F}{\delta a}\right) \geq \mathcal{G}_{IC} \tag{3.33}$$

This provides an expression for the strain energy release rate in terms of measurable parameters, F, D, and their derivatives with respect to the crack length. We can make this equation an equality and by doing so, we make the measureables F and D into F_C and D_C, the critical force and displacement for crack growth. Thus,

$$\frac{1}{2w}\left(F_C\frac{\delta D}{\delta a} - D_C\frac{\delta F}{\delta a}\right) = \mathcal{G}_{IC} \tag{3.34}$$

Examination of Figure 2.6 provides a way we can make Eq. (3.34) into an expression that measures one variable instead of two. If the axes of Figure 2.6 were in terms of stress and strain, the slope of the line would be the modulus. However, since the axes are force and displacement, we may say only that the slope of the line is the *stiffness* of that particular specimen. The inverse of the stiffness is the pliability or the *compliance* of the specimen. $C = D/F$, because we are dealing with linear elastic materials, where C is the compliance. Using this expression, we can simplify the equation for the critical force and displacement for crack growth:

$$\frac{D_C^2}{2W}\frac{1}{C^2}\frac{\delta C}{\delta a} = \frac{F_C^2}{2w}\frac{\delta C}{\delta a} = \mathcal{G}_{IC} \tag{3.35}$$

This last equation is important because the quantity $\delta C/\delta a$ can either be calculated or measured. For double cantilever beams, the quantity $\delta C/\delta a$ can be determined from beam theory. For a beam of uniform cross section, height h, width w, and modulus E, the change in compliance with crack length is found to be:

$$\frac{\delta C}{\delta a} = \frac{8}{Ew}\left(\frac{3a^2}{h^3} + \frac{1}{h}\right) \tag{3.36}$$

This equation says that we can make $\delta C/\delta a$ a constant if the quantity in the parentheses is a constant. This was accomplished and researchers generated height-or width-tapered double cantilever beams. A height-tapered, double cantilever beam has been used in the examination of structural adhesives with aluminum adher-

ends, while a width-tapered, double cantilever beam has been used to study adhesive-bonded, carbon fiber-reinforced composites [9]. Depending on the Young's modulus of the adherends, different tapers are used to produce specimens of appropriate dimensions. The determination of $\mathcal{G}_{IC}$ is made simpler by using tapered beams because the critical strain energy release rate is directly related to the critical force for crack propagation. Figure 3.18 shows a comparison of F–D plots for the determination of $\mathcal{G}_{IC}$ for both uniform and tapered, double cantilever beam specimens.

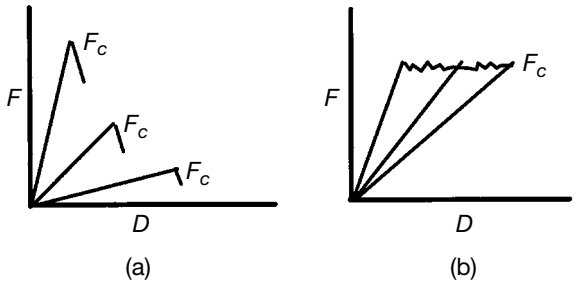

Figure 3.18 Schematic diagram of force-displacement curves measured for a double cantilever beam specimen. (a) Shows a result for a uniform, double cantilever beam. (b) Shows a result for a tapered, double cantilever beam. Note that the critical force for crack growth is easily determined from the force-displacement curve from a double cantilever beam

Examination of the curves in the two sides of Figure 3.18 demonstrates how the data from the two specimens differs. Figure 3.18(a) shows the data obtained for a uniform double cantilever beam. Each straight-line section is associated with loading the specimen until a crack begins to propagate. When the specimen is reloaded, the compliance has changed (the length of the lever arm is longer) and the reloading curve is different. In each case, a different F_C is measured. These F_Cs correspond to the same $\mathcal{G}_{IC}$, which can be calculated from each measured F_C when the F_C is corrected for $\delta C/\delta a$. It is obvious from Figure 3.18(b), that the tapered specimen provides a constant F_C no matter what the crack length was when it was measured. The tapered specimen provides a direct measure of $\mathcal{G}_{IC}$.

3.5.2 Blister Test

There are a number of other specimens used to determine the critical strain energy release rate of an adhesive. One method described by Dannenberg[10] is called the "blister test". It involves the use of a plate through which a hole has been drilled. A schematic of this apparatus is shown in Figure 3.19. The hole is covered by poly(tetrafluoroethylene) tape or other release material and the adhesive as well as

4.2.2.1 Dipole–Dipole Interactions

Each element in the periodic table can be characterized by how much it attracts electrons. Thus, elements on the right hand side of the periodic table are said to be *electronegative* in comparison to the elements on the left-hand side of the periodic table. When atoms are bound together to make molecules, the electronegativity of the individual atoms acts to draw electrons towards those that are the most electronegative. Thus, a molecule such as CF_3CH_3, with the very electronegative fluorine atoms on one end of the molecule, has more of the electron density in the molecule residing more on one end than on the other. One could say that there was a partial charge on either end of the molecule. The CF_3 side has a partial negative charge and correspondingly, the CH_3 end has a partial positive charge. In terms of quantum mechanics, the probability function for the electron is greater in the region around the fluorine atoms than it is around the hydrogen atoms. This type of molecule, with a partial separation of charge is known as a *dipole*.

The dipole is characterized by the magnitude of the virtual charge on the ends of the molecule as well as by the distance separating the virtual charges. It is usual to draw a dipole as a dumbbell. The charges reside in the "balls" of the dumbbell. The handle of the dumbbell is the length separating the charges. The dipole is able to act in a mechanical way. If an interaction occurs between a singly charged species and a dipole, the opposite charges attract and the negative charges repel according to Coulomb's Law. The line of action of this force is controlled by the "lever" holding the virtual charges together. A force acting on a lever in this way is a "moment" and for this situation, we can define a *dipole moment,* μ:

$$\mu = q\,l \tag{4.10}$$

where q is the magnitude of the virtual charge, and l is the molecular length separating the charges.

Two dipoles can interact. The oppositely charged ends of the dipole attract and the similarly charged ends of the dipoles repel, thus changing the spatial orientation of one with respect to the other. Figure 4.1, shows such a situation. The potential energy of interaction of two dipoles becomes a matter of trigonometric analysis of charges and moments acting upon one another. This dipole-dipole potential energy of interaction is written as follows:

$$\boldsymbol{\Phi}^{\mathrm{p}} = \frac{\mu_1\mu_2}{r^3}\left[2\cos\theta_1\cos\theta_2 - \sin\theta_1\sin\theta_2\cos\left(\phi_1 - \phi_2\right)\right] \tag{4.11}$$

where μ_1 and μ_2 are the dipole moments and r is the distance of separation of the centroids of the two dipole moments [2]. The angles are all shown in Figure 4.1.

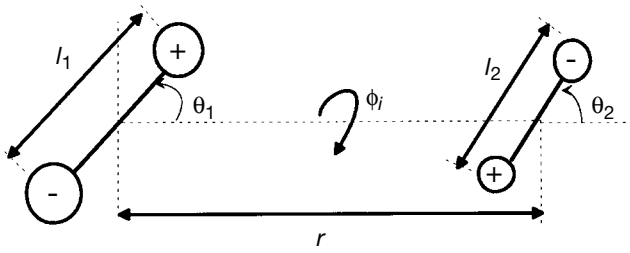

Figure 4.1 Diagram showing the interaction between two dipoles. The interaction is specified by the angles of orientation as well as by the dipole moments of the two molecules

An important advancement concerning the understanding of dipolar species came with the work of Keesom [3]. He surmised that dipoles in a liquid or gas did not exist as species rigidly fixed with one another. Rather, if a liquid or a gas is at a temperature such that its thermal energy is greater than the rotational energy of the dipoles in that material, then the dipoles are free to rotate with respect to one another. The potential energy of interaction must be averaged over all values of θ and ϕ to provide a thermally averaged interaction. Keesom derived the following expression for the potential energy of interaction for rotating dipoles with an average thermal energy of $k\,T$, where k is Boltzmann's constant and T is the absolute temperature:

$$\boldsymbol{\Phi}^{\mathrm{P,K}} = -\frac{2\mu_1^2\mu_2^2}{3kTr^6} \tag{4.12}$$

Other constants in the equation were described previously. An adhesive, when applied, is almost always a liquid and may be described by a Keesom potential, although it is somewhat dubious for us to assume that the interactions that occur between a solid adherend and a liquid adhesive would best be described this way. The Keesom potential may be a reasonable approximation.

4.2.2.2 Dipole-Induced Dipole

In another type of van der Waals interaction between molecules, greater attention is given to the interaction of the electron clouds surrounding molecules. When a molecule with a spherical, symmetrical charge distribution encounters a dipole, we might expect no interaction between these molecules. However, this is not the case. There is a measurable interaction between the two molecules, called the *dipole-induced dipole* interaction. This interaction occurs because of the nature of electron probability distributions around the nuclei in a molecule. We know from atomic theory that electrons move in molecular orbitals and these molecular orbitals can interact with other charges, changing the probability distribution of the electron in its orbital. Simply stated, the electrons in a spherical, symmetrical molecule see the dipole as two charges. The electrons are attracted to the positive

essentially all polymers have similar glassy moduli of about 3×10^9 Pascal. Above the glass transition temperature, the material first behaves tough or leathery and at higher temperatures, behaves as an elastomer. The modulus of the material decreases substantially above the T_g. Another way of determining the glass transition temperature of a polymer is to measure the stress-strain properties as a function of temperature. Although effective, this set of data is quite tedious to collect. For many adhesive materials, the maximizing of adhesive properties in the temperature range between T_g and T_m or the decomposition temperature of a thermoset is the goal of the adhesive formulator.

■ 5.4 Dynamic Mechanical Measurements and Viscoelasticity

In Chapter 2, we defined the complex modulus of a viscoelastic material as well as the storage and loss moduli. That description provided the basis for linear viscoelasticity, but it did not provide a discussion of the means by which we measure these properties. In this section, methods through which these properties can be measured are described. The measurement of the viscoelastic properties of polymers by the application of a sinusoidal stress is known as *dynamic mechanical spectroscopy*.

5.4.1 Methods of Measurement of Dynamic Mechanical Properties

A schematic diagram of an instrument for the measurement of dynamic mechanical properties is shown in Figure 5.4. The diagram is an extremely simple version of the many complicated devices of this type now available. A sample of polymer is firmly clamped between two pieces of metal that are much stiffer than the sample. One of the clamps is connected to a sinusoidal driving device while the other is connected to a force transducer. The instrument should be capable of measuring both the frequency and the amplitude of the driven and transduced signals. The resulting data can then be analyzed as described in Chapter 2. An important feature (which was not emphasized in Chapter 2) is that dynamic mechanical measurements are done as a function of temperature (at a single frequency) or frequency (at a single temperature). The most versatile instruments of this type can carry out the measurement both of these ways. The reasons for the importance of this statement are made clear in this and later chapters.

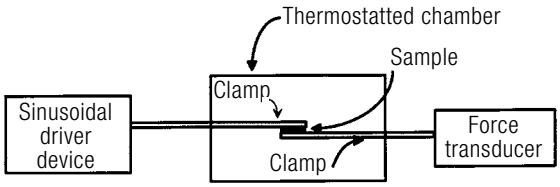

Figure 5.4 Diagram of a simple dynamic mechanical spectrometer used to measure the shear properties of a material. Note that a sinusoidal driver device is used. Frequency and temperature are controlled. The stiffness of the device must exceed that of the sample for the measurements to be valid

The sample configuration shown in Figure 5.4 is analogous to the lap shear specimen discussed in Chapter 3. The measurement done in this mode provides the shear storage and loss moduli. The measurement can be carried out so that the sample is suspended between the two clamps. The measurement is then in tension and the corresponding Young's moduli are determined. The sample must be stiff enough at the temperature and frequency range of interest, so that it does not slump or change shape during the measurement.

Another important means to make dynamic measurements is by a rotating or oscillating rheometer. A schematic of a sample configuration for such a rheometer is shown in Figure 5.5. The sample is placed in a state of shear. The complex shear modulus can be determined by the application of an oscillating sinusoidal stress. This instrument is also useful for determining the viscosity of a material as a function of shear rate, which is controlled by the rate of revolution of the upper spindle. Yield stresses of fluids can be measured as a function of temperature as well. This last measurement is important in the design of materials with non-sag characteristics.

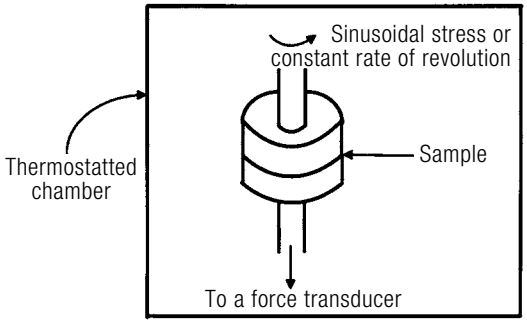

Figure 5.5 Simplistic diagram of the sensor head in a rotating viscometer. Note that in this configuration the sample is in pure shear

The last dynamic mechanical spectrometer discussed here is the torsion pendulum. This spectrometer was well researched by Gilham and his group at Princeton University [1]. A schematic of the apparatus is found in Figure 5.6. A device that provides the spin also holds the sample. The spin is transmitted through the sample and the specimen rotates. When the spin is abruptly released (analogous to the wind-up and release of a mainspring), the response of the specimen to the initial perturbation is determined by watching the decay of the resulting oscillation.

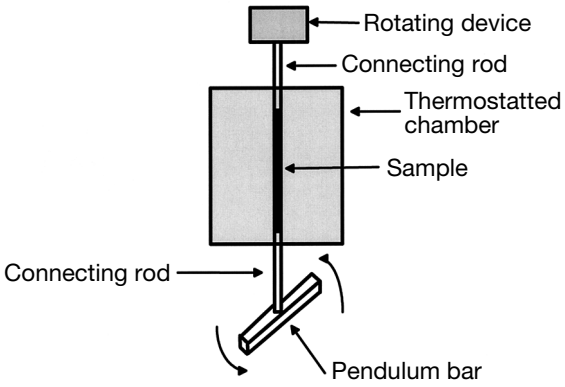

Figure 5.6 Schematic diagram of a torsion pendulum device used to measure dynamic mechanical properties of a polymer. If the sample is generated using a braid into which a thermoset polymer has been impregnated, the device can be used to measure the cure rate and the change in physical properties as a function of cure time

The oscillation can be observed in any one of a number of different ways. For example, on the bottom of the pendulum, a disk can be placed upon which is a digital code for position. A bank of lights and photodiodes can read the digital code. An exponentially damped sinusoidal curve results. The measured quantities are the frequency of oscillation and the decrease in the amplitude of the oscillation as a function of time (damping). This is not a direct measurement of modulus. The frequency of the oscillation is related to the stiffness of the material and the decrease in amplitude per cycle is related to the energy lost by the sample. The tan δ can be determined from this measurement. If G' or G'' has been determined independently, the other can be determined with tan δ. The apparatus shown in Figure 5.6 has not found as much use as the other instruments described earlier because the actual Young's or shear moduli cannot be determined directly. The apparatus is, however, very useful for the study of the cure processes of thermosetting materials.

A glass braid can be impregnated with a thermosetting polymer. The braid is then placed in a thermostatted compartment in the torsion braid analyzer. The sample is heated and the stiffness of the sample is determined as a function of time. Gilham has made good use of this type of analysis in his description of T–T–T plots

Surface topography of copper foil		Mean peel load lb/in
Topography	Diagrammatic representation	
Flat		3.75
Flat + 0.3 μ dendrites		3.8
Flat + 0.3 μ dendrites + oxide		4.4
3 μ pyramids (high angle)		5.9
2 μ low angle pyramids + 0.3 μ dendrites		7.3
2 μ low angle pyramids + 0.2 μ dendrites + oxide		8.8
3 μ high angle pyramids + 0.2 μ dendrites + oxide		13.5

Figure 6.9 Experimental results reported by Arrowsmith, relating the surface roughness of electroplated copper to the level of practical adhesion when an epoxy adhesive is removed. Note that as the level of surface roughness increases and the opportunity for mechanical interlocking increases, the level of practical adhesion increases even though the adhesive is identical in all cases (reproduced from Reference 11 by permission of the Institute of Metal Finishing, UK)

6.5.1 Kinetics of Pore Penetration

The above discussion is predicated on the notion that the adhesive and the adherend are in intimate contact. It is not obvious that this should be the case since all real adhesives have a viscosity. In normal bonding operations, the adhesive and adherend must come into close contact quickly. We can examine the extent to which adhesives penetrate into pores on a surface by examining the equations describing the wetting of surfaces by polymers and the penetration of liquids into a pore as provided by Packham [12]. Poiseulle's Law describes the penetration of a liquid into a pore:

$$x\frac{\mathrm{d}x}{\mathrm{d}t} = \frac{r^2 P}{8\eta} \tag{6.8}$$

where x is the pore penetration distance, P is the capillary pressure, t is the time, and r is the radius of the pore (or capillary, for which Poiseulle's Law is actually derived). The capillary pressure is given by:

$$P = \frac{2\gamma_{\mathrm{LV}}\cos\theta}{r} \tag{6.9}$$

where θ is the contact angle and γ_{LV} is the liquid-vapor interfacial tension of the adhesive. The description of the wetting of a surface by a polymer is taken from the work of Schonhorn, Frisch, and Kwei [13] and it is described by the following equation which was derived by Newman [14]:

$$\cos\theta(t) = \cos\theta_{\infty}\left(1 - a e^{-ct}\right) \tag{6.10}$$

where θ_{∞} is the contact angle at infinite times and $\theta(t)$ is the time dependent contact angle. Combining these equations, we find the following relationship:

$$x^2(t) = \frac{r\gamma_{LV}\cos\theta_{\infty}}{2\eta}\left(t - \frac{a}{c} + \frac{a e^{-ct}}{c}\right) \tag{6.11}$$

This equation describes the distance a pore is penetrated by an adhesive, giving an idea of the parameters necessary for expulsion of air from a pore and its replacement by an adhesive.

Let us examine the above equation by introducing parameters associated with the wetting of a surface by polyethylene. Packham assumed that the interfacial tension between the polyethylene and air was 23.5 mJ/m^2 under the application condition which was 200 °C. He allowed a time of 20 minutes for wetting to take place. Table 6.1 shows results of his calculations.

Table 6.1 Packham's Calculation of Distance Penetrated by Molten Polyethylene into a Microporous Surface

Pore radius (micrometers)	Distance penetrated into pore "x" (micrometers)
1000	220
10	22
1	7
0.1	2.2
0.01	0.7

The table clearly indicates that the amount of penetration of polyethylene into a porous surface is dependent upon the radius of the pore. The depth of penetration is inversely dependent upon the radius of the pore. For a pore radius of 1,000 microns, the depth of penetration is only 220 microns. If the pore were as deep as its radius, the pore would still be mostly empty. In contrast, if the pore radius were 0.1 microns, the depth of penetration could be 2.2 microns, if the pore had that depth available. The calculation clearly says that if we wish to have as complete as possible removal of air from a pore on a surface, the pore radii must be quite small. The approximate radii of the openings of pores that are deeply penetrated are about one micron or less. The ramifications of this correlation become clearer when we discuss surface preparations in the next chapter.

Thus, another criterion for obtaining *good adhesion is provide a surface with a micro-morphology and provide an adhesive with a low enough viscosity to completely fill the surface features.*

■ 6.6 Wettability and Adhesion

Examine Figure 6.10 and imagine a situation in which there is a real adhesive and a real adherend. The importance of wettability to adhesion is apparent. A tortuous surface like that in Figure 6.8 is not necessarily completely clean. Contaminants are likely to be on the surface, forming a "weak boundary layer" (see Section 6.9). In addition, a real adhesive has a real viscosity (as discussed in the previous section). In many cases, the adhesive will need to cure and the viscosity in these materials increases rapidly as a function of time after application. We can expect that the bottom of the pores may not be filled, leaving voids. The adhesive bond may therefore have vacancies at the interface, each of which acts as a stress concentration point. To understand this problem, re-examine Figure 1.1. We show two situations, one is a perfect monolithic material in which there are no cracks or voids and the other is of the same material containing a crack.

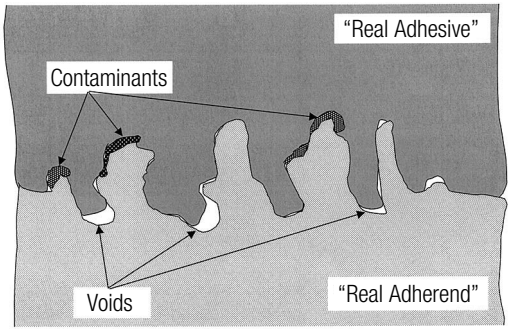

Figure 6.10 Schematic of a "real" bonding situation in which the surface of the adherend has contaminants and in which the adhesive has a finite viscosity. Pore penetration is not complete, leaving voids at the interface. The presence of voids as well as cohesively weak contaminants, decreases the strength of the adhesive bond below its theoretical strength

We can imagine a load being placed on both samples. The load is shown propagating through the unflawed material as continuous lines of force. In the flawed material, the lines of force cannot be continuous because of the flaw. The lines of force, because they must be continuous, gather at the edge of the flaw and increase in intensity. The increase in intensity can be calculated in a simple way for this ellip-

rusting. If the corrosion products are weakly adhered or cohesively weak, the surface preparation is spoiled.

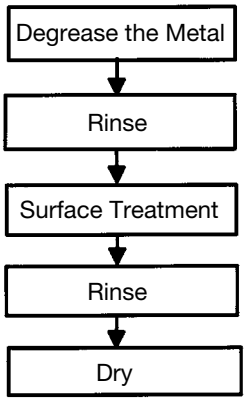

Figure 7.9
Flow chart for the surface preparation of metals

Similar problems occur in using abrasive surface preparation methods for metals. If the metal is very oily, the abrasive can just drive the oil deeper into surface crevices. Thus degreasing is necessary before an abrasive surface treatment, just as it is before an electrochemical surface treatment. Rinse steps are also important, as debris left on a surface can act as a weak boundary layer or particulates can act as stress concentration points, weakening the overall structure. Once rinsing is used, drying becomes important for the reasons expressed earlier.

7.3.1 Surface Preparation of Aluminum for Adhesive Bonding

We begin with the discussion of surface preparation of aluminum because there is more literature available on this metal than for any other metal. In addition, the surface preparation of aluminum is more critical than that for other metals in that this metal is used for many aerospace applications (see Chapter 1). We have already used aluminum as an example of a material that is thermodynamically unstable under normal atmospheric conditions, but that becomes useful because of a kinetic barrier to its instability, aluminum oxide (see Chapter 6). The basis for the surface preparation of aluminum is the creation of an oxide not only amenable to adhesive bonding, but also stable under the conditions to which the adhesive bond is exposed.

7.3.1.1 The Forest Products Laboratory (FPL) Etch

The FPL treatment for aluminum was first described by Eickner [40] who worked at the Forest Products Laboratory in the early 1950s. This treatment consisted of immersing aluminum in a solution similar to the chromic/sulfuric acid solution discussed in the section on wet chemical treatment of polymers. Possibly unknown

to the developers of this surface treatment method, the action of chromic acid and sulfuric acid on aluminum was more than just the oxidation of organic contaminants on the surface. The treatment was electrochemically active with aluminum. A standard surface preparation method incorporating the FPL procedure is shown in Figure 7.10.

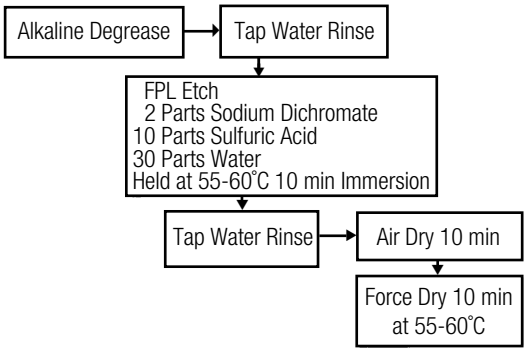

Figure 7.10 Flow chart for the FPL process for the surface preparation of aluminum

There are many variations of the FPL etch. In Europe, this treatment is known as chromic acid "pickling". In the pickling treatment, chromic acid is used instead of sodium dichromate and often, deionized water is used instead of tap water. The FPL etch was used in the aerospace industry with great success after the end of World War II, when phenolic-based primers and structural adhesives were the norm.

As was mentioned in Chapter 1, structural adhesives are used extensively in the generation of honeycomb structures. Phenolic structural adhesives cannot be used in this application because the high-pressure requirements for their proper cure crush the honeycomb core (see Chapter 8). Luckily, at about the time this application arose, epoxy-based structural adhesives were developed. Epoxy-based structural adhesives did not require high pressures for wetting and curing. Epoxy structural adhesives became widely used in honeycomb structure as well as for metal-to-metal bonding with the FPL etch as the primary surface preparation. The timeframe was the 1960s and many aircraft were deployed in Viet Nam. Under the conditions of high temperature and high humidity encountered by aircraft in that conflict, adhesive bonds failed. In addition, the Boeing Corporation found adhesive disbondments and corrosion in several of their aircraft. The aircraft industry started a significant amount of research and development work at this time to determine the cause of the failures.

A significant advance was made when Boeing engineers heeded the words of their shop workers who said that "new" FPL etch baths did not give satisfactory performance. However, if the bath was allowed to age, performance increased substantially.

After considerable effort, it was found that the addition of 2024-T3 aluminum alloy to the FPL etch substantially improved the performance of adhesive bonds that were surface prepared with this etch and bonded with an epoxy. It was later shown that the action of the added 2024-T3 provided copper (copper is an ingredient of 2024-T3 alloy) [41]. The addition of copper modifies the electrochemistry of the FPL etch, making the metal surface more noble and, in fact, inducing an oscillating electrochemical reaction in which the copper participated [42]. The action of the bath was to induce a structure in the oxide on the surface of the alloy. An electron micrograph of the FPL oxide structure is shown in Figure 7.11 and a drawing of the structure is shown in Figure 7.12. Note that the oxide structure seems designed for adhesive bonding. The pores on the surface are small (to help with capillary forces that could displace air). The surface is clean. If the bath is properly maintained, the surface is reproducible. Examination of the chemistry of this oxide by various analytical tools showed that the oxide was essentially pure Al_2O_3. Under the oxide, however, some amount of copper could be found. This demonstrates copper's participation in the electrochemistry of formation of the oxide [42].

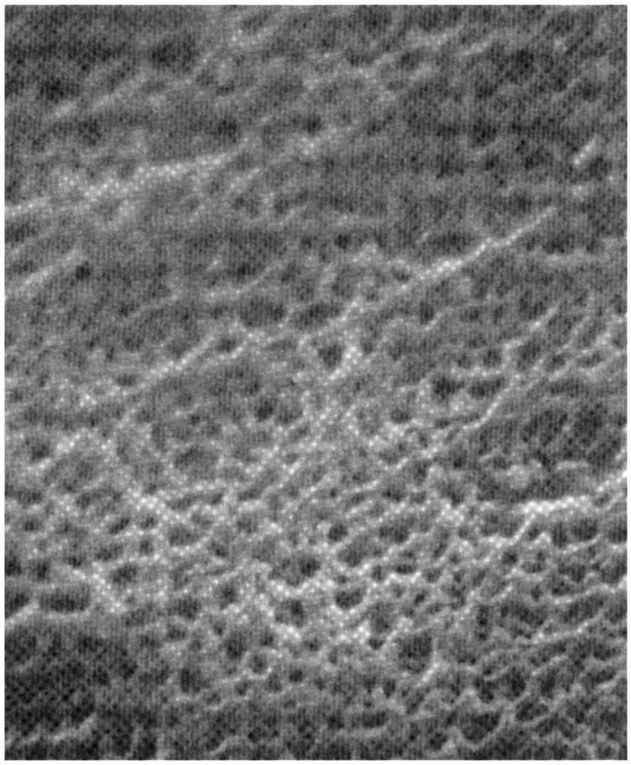

Figure 7.11 Electron micrograph of an aluminum surface generated by treating the aluminum with an FPL etch process. The magnification is 80,000×. Note the porosity of the surface. Compare this micrograph with the schematic drawings in the next figure

but the advantages in terms of high and low temperature performance, as well as their hypoallergenic character, can often outweigh the extra cost. We will discuss other types of silicone-based adhesives in more detail in the section on rubber-based adhesives.

Poly(iso-butylene), polyvinyl ethers, and polybutadiene can also be made into PSAs. The structures of these three polymers are also shown in Figure 10.1. In comparison to the other classes of PSA base elastomers, these three form the smaller portion of the market. Polyvinyl ethers were once thought to provide performance equivalent to that of the polyacrylates. However, the polyvinyl ethers had a feel of "dry tack" which did not provide the "thumb appeal" that the acrylates exhibited. Polyvinyl ethers are usually not modified with tackifiers, but rather are blends of high and low molecular weight polymers. Poly(iso-butylenes) are unique polymers in terms of their resistance to oil as well as their low moisture permeability. Because of its saturated chemical character, these polymers are weatherable. Similarly, they are difficult to crosslink and thus exhibit poor shear characteristics. Poly(iso-butylenes) are tackified to achieve performance. Polybutadiene can be made into a PSA and it is eminently crosslinkable. Combined with its low glass transition temperature and good electrical properties, this material has found use in electrical tapes.

10.2.2 Chemistry of Tackifiers

Tackifiers are a unique class of materials. They normally have low molecular weight and are resinous, but yet they have glass transition and softening temperatures often much above room temperature. It is this combination that makes these materials useful in the formulation of PSAs. Tackifying resins are usually based on natural products or petroleum streams. In the following discussion, these materials are classified according to the materials from which they are synthesized.

10.2.2.1 Natural Product Based Tackifiers

Rosin acid derivatives are the oldest known tackifiers. The structures of abietic acid and pimaric acid, which are components of rosin, are shown in Figure 10.2. Abietic acid itself can be used as a tackifier, but most often the material is chemically modified in some way. The unsaturation of abietic acid can be expected to lead to oxidation and discoloration. Hydrogenation of those double bonds can eliminate that problem. Rosin acid is also used in esterified form. Typically, abietic acid is esterified with glycerol or pentaerythritol to generate higher softening point materials. Rosin acids are obtained as wood by-products such as gum rosin, wood rosin, and tall oil. Rosin acid and their esters are most often used in the formulation of natural rubber-based PSAs.

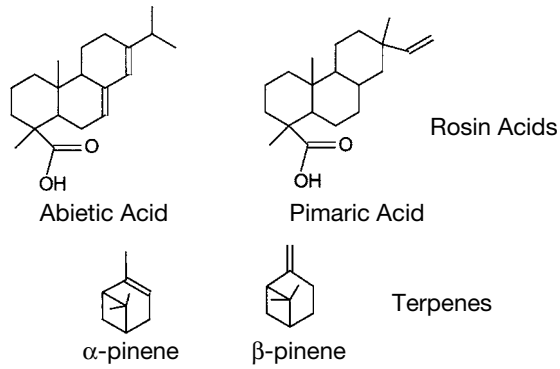

Figure 10.2 Chemistry of rosins and terpenes

Another natural product based tackifier is that based on α- or β-pinene whose structures are also shown in Figure 10.2. This class of materials is known as the "terpenes". α- or β-pinene is usually used in the polymerized state. The polymerization is done cationically by aluminum chloride catalysis. The softening point of this resin strongly depends upon its molecular weight and is remarkably high for a low molecular weight material. For example, at a molecular weight of about 1,200, the softening point can be about 120 °C. Terpenes are obtained from citrus peels or wood by-products.

10.2.2.2 Petroleum Based Tackifiers

Since petroleum is a natural product, it is difficult to classify the next set of resins as being "synthetic". This class of tackifiers is differentiated from those described above in that they are obtained from petroleum cracking products and not directly from flora. Petroleum-based tackifiers are also not used as obtained from the petroleum stream. They are polymerized to raise their softening points to the level that they become useful in PSAs. The same process used to polymerize β-pinene resins is used for petroleum-based tackifiers. These tackifiers are broadly classed into two types, the aromatic and aliphatic resins. The aromatic resins are further classified into coumarone-indene resins, aromatic petroleum resins, and heat reactive resins. The aliphatic resins are also known as "C-5" resins since much of their chemistry revolves around polymerized pentene and cyclopentene.

The structures of the compounds used in coumarone-indene aromatic resins are shown in Figure 10.3 as are those used in the aromatic petroleum resins and the heat reactive resins. Cationic polymerization of combinations of these compounds leads to a large class of materials. The coumarone-indene resins and the aromatic resins are often used with natural rubber-based adhesives. Care must be taken in the formulation of block copolymer-based PSAs to insure that the tackifier does not dissolve in the polystyrene phase. The cohesive properties of block copoly-

mer-based adhesives depend upon the phase separation and glassy nature of the polystyrene phase. If the polystyrene phase is not glassy, the effect of the phase-separated particle is diminished. The aromatic resins discussed here are most likely not useful in block copolymer-based adhesives, since their solubility properties are similar to the polystyrene phase and would thus plasticize that phase. The C-5 resins, which are more compatible with the polyisoprene phase, are more likely be used in block copolymer-based PSAs.

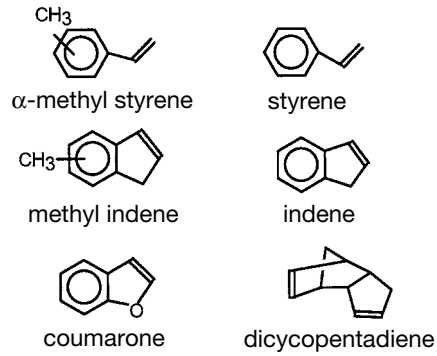

Figure 10.3 Chemistry of materials used to make petroleum-based aromatic tackifiers

The chemical structures of the monomers used in the generation of C-5 aliphatic resins are shown in Figure 10.4. Once again, these materials are copolymerized in various ratios using aluminum chloride catalyzed cationic polymerization. The aliphatic resins have no tendency to yellow as would the aromatic materials discussed earlier. These resins are used in natural rubber-based PSAs as well as the block copolymer-based PSAs. Even though we have classified tackifiers in a certain way, aliphatic-aromatic resins as well as C5–C9 resins can be made by taking materials from the two streams and copolymerizing them. Table 10.1 provides a listing of a number of tackifying resins, their classification, molecular weights, and softening temperatures.

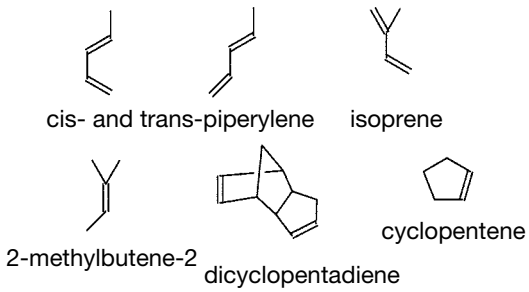

Figure 10.4 Chemistry of materials used to make petroleum-based C-5 tackifiers

11.5 Thermoplastic or Pseudo-thermoplastic Adhesives Based upon Natural Products

The oldest adhesives are based upon natural products. The use of proteins as base resin for a structural adhesive was described in an earlier chapter. However, a number of other natural product-based materials are also used as adhesives or as adhesive components and some are discussed in this section.

11.5.1 Starches [7]

Starches are obtained from roots and seeds and we classify them as pseudo-thermoplastic materials, because starch is not actually soluble. Rather, starch is a branched polysaccharide consisting of amylose and amylopectin (structures are shown in Figure 11.7). Since starches are highly branched, they are not soluble in water and most other materials. Because of their chemical structure, they swell considerably in water, particularly when the water is boiling. The water-swollen starch particles behave like a pseudoplastic emulsion that can be coated onto paper as well as other substrates to act as a re-moistenable adhesive. Starches can be formulated with a number of materials as plasticizer, such as glycerol, corn syrup or molasses. Borax is important in starch-based adhesives because it acts as a rheology modifier and at sufficiently high concentrations, as an anti-microbial.

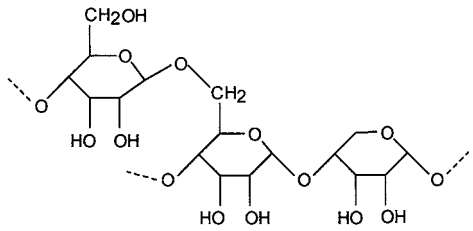

Figure 11.7 Structure of amylopectin

11.5.2 Cellulosics [8]

The feedstock for cellulosic adhesive materials is wood pulp and cotton linters with the second providing higher quality cellulose. A good way to describe the possible uses of cellulosics in adhesive technology is by the diagram shown in Figure 11.8. Cellulose, because it is inherently insoluble, must be chemically modified to make

useful adhesives. The oldest form of chemical modification is nitration. Reaction of cellulose with approximately a single nitration per ring yields cellulose nitrate. This form of cellulose is soluble in such solvents as amyl ketone and toluene. The solvated form of nitrocellulose is the well-known adhesive; Duco[1] Cement sold for many years by the DuPont Company. Esterification of cellulose leads to cellulose acetate or triacetate. One use of these materials is used for very clear, thin film products ("celluloid" or "cellophane"). These products formed the base for photographic films before the advent of polyethylene terephthalate and served as the backing for many pressure sensitive adhesive tapes. Etherification of cellulose yields hydroxyethyl and hydroxy methyl cellulose. Their utility as protective colloids for emulsions, including those based upon PVAc, has been described. Hydroxymethyl cellulose also forms the basis for many wallpaper adhesives.

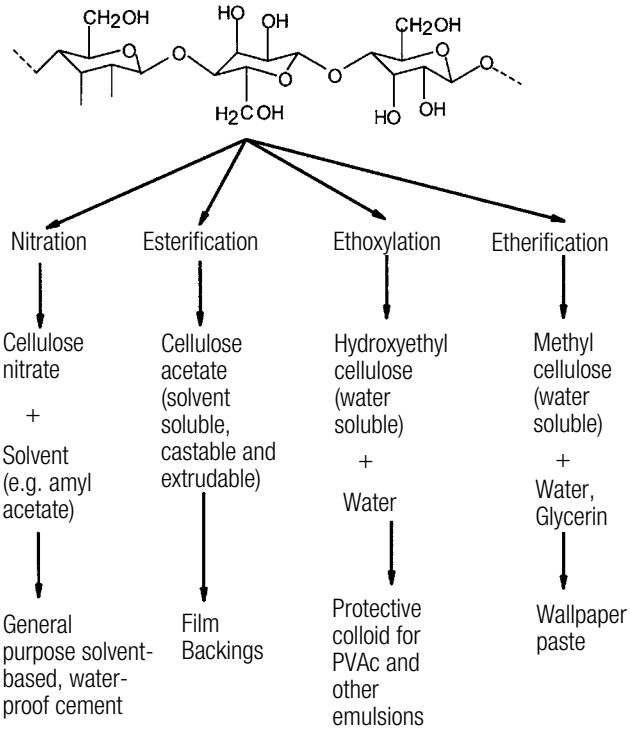

Figure 11.8 Reactions used to modify cellulose to yield useful adhesive products

[1] Duco is a trademark of E.I. DuPont de Nemours Co.

■ 11.6 Summary

In this chapter, the chemistry of a number of adhesives classified as thermoplastic or pseudothermoplastic has been described. Most of the adhesives in this chapter start out as primarily thermoplastic but often are modified to be crosslinkable to impart properties such as creep and solvent resistance. The primary types of adhesives discussed are hot melts, emulsion adhesives, polyvinyl acetal adhesives and natural product-based adhesives. In general, these adhesives are moderate in strength with shear performances that are somewhat higher than that of rubber-based adhesives but substantially less than structural adhesives.

■ Bibliography

Handbook of Adhesives, 2nd ed. Skeist, I., (Ed.) (1977) Van Nostrand Reinhold, New York

Weidener, R. A., in Treatise on *Adhesion and Adhesives,* Vol. 2. Patrick, R. L. (Ed.) (1969) Marcel Dekker, New York

Carpenter, A. T., Taylor, J. R., in *Adhesion 1. Allen,* K. W. (Ed.) (1977) Applied Science Publishers, London

■ References

[1] Litz, R. D., *Adhesives Age* (August 1972) pp. 44–46

[2] Shih, H-H., Hamed, G. R., *J. Appl. Polym. Sci.* (1997) 63, p. 323

[3] Shih, H-H., Hamed, G. R., *J. Appl. Polym. Sci.* (1997) 63, p. 333

[4a] Hardy, A., in *Synthetic Adhesives and Sealants*. Wake, W. C. (Ed.) (1986) John Wiley, Chichester

[4b] Flory, P. J., *J. Chem. Phys*. (1949) 17, p. 223

[5] Rossito, C., in *Handbook of Adhesives*. Skeist, I. M. (Ed.) (1990) Van Nostrand Reinhold, New York, pp. 478–498

[6] Cowan, J. C., *J. Am. Oil Chemists Soc*. (1962) 39, p. 534

[7] Williams, R. H., in *Modified Starches, Properties and Uses*. Wurzburg, O. (Ed.) (1987) CRC, Boca Raton, FL

[8a] Hon, D. N-S., in *Adhesives from Renewable Resources*. Hemingway, R. W., Conner, A. H., Branham, S. J. (Eds.) (1989) American Chemical Society, Washington, DC

[8b] Wint, R. F., Shaw, K. G., in *Applied Polymer Science*. Tess, R. W., Poehlein, G. W. (Eds.) (1985) American Chemical Society, Washington, DC

[8c] Nicholson, M. D., Merritt, F. M., in *Cellulose Chemistry and its Applications*. Nevell, T. P., Zeronian, S. H. (Eds.) (1985) Ellis Horwood, Chichester, UK

Index